PROTEIN RELEASE FROM DIFFERENT FORMS OF POLYLACTIDE AND ALGINATE COMPOSITE CARRIERS

Anna Morawska-Chochół*

AGH University of Krakow,
Faculty of Materials Science and Ceramics,
Department of Biomaterials and Composites,
al. A. Mickiewicza 30, 30-059 Krakow, Poland
*e-mail: morawska@agh.edu.pl

Abstract

The development of composite biomaterials constituting both a porous scaffold for filling tissue defects (especially bone tissue) and a carrier of biologically active substances (proteins) is an innovative approach of the presented research. The paper presents the following studies of obtained composites: model protein (bovine serum albumin, BSA) release, changes in microstructure during incubation and bioactive potential in a simulated biological environment (based on scanning electron microscopy with X-ray microanalysis – SEM/EDS – and infrared spectroscopy – FTIR). Three types of composites with a poly(L-lactide) matrix PLLA were investigated. PLA fibres covered with silica-calcium sol, calcium alginate fibres and calcium alginate beads were used as modifiers of the PLA matrix and carriers of protein. Process of releasing albumin proceeded differently depending on the material and form of the carrier. In the case of calcium alginate fibres, almost all protein was released within 14 days. For the remaining materials, this amount was reached after 3 weeks. All tested composites showed bioactive potential connected with apatite precipitation during incubation in a simulated biological environment. However, coating PLA fibres with silica-calcium sol significantly increased this effect. The highest cell viability was observed for a biomaterial modified by calcium alginate beads.

Keywords: *polylactide, calcium alginate, bovine serum albumin, protein release, bioactive composite, multifunctional composites*

Introduction

Due to trauma in life, regeneration of lost tissue such as bone, cartilage, skin, muscle, and tendons is still an actual problem. Grafts for filling large defects are one of the ways to heal and regenerate tissue [1,2]. Scaffolds which can deliver biologically active reagents stimulating growth of the treated tissue are a new conception [3]. This solution must combine a surgical implant with a drug carrier. Such a complex function increases the requirements for this type of biomaterial. On the one hand, it must perform a structural function, allowing the restoration of natural biomechanics thanks to appropriate mechanical parameters, and during the healing time undergo controlled degradation, allowing overgrowth of tissue through the implant. On the other hand, proper biological action is desirable, serving to activate and stimulate regenerative processes by providing the appropriate proteins, growth factors, enzymes, or drugs. The most popular materials for the delivery of biologically active substances are degradable polymers, such as polylactide and alginate [4-6]. Alginates are immensely popular hydrogels due to their biocompatibility, similarity to the natural extracellular matrix, high swelling capacity and low costs of production. However, too fast diffusion of the delivered drug is often a problem in alginate carrier application [7]. The controlled release can be realized by chemical modification of alginate beads by hydrophobic materials in the form of a coating or incorporation of organic compounds into alginate beads to create a hydrophobic gel matrix [7]. The poor mechanical parameters of alginate significantly limit the possibilities of their application.

Polylactides (PLAs) are also popular materials in drug delivery. Common forms in these applications are nano- and microcapsules or nonwovens [6,8-10]. Their only function is the controlled delivery of biologically active agents, and mechanical stabilization cannot be realized. Other forms of PLAs, such as fibres or scaffolds, are also being developed in the current research [11-13]. PLA and its copolymers, thanks to relatively good mechanical parameters and the ability to control the time of their degradation, are widely used as scaffolds in tissue engineering. The desired scaffolds microstructure can be controlled by selecting the appropriate technology (electrospun mats, 3D printing, freeze-drying) [14-16]. The creation of PLAs-matrix composites also allows them to be strengthened mechanically (especially by fibre modification) and gives them additional properties, such as bioactivity (hydroxyapatite or bioglass additives for healing of bone defects) [16,17]. Such properties are particularly important in the case of grafts intended to fill bone tissue defects. Bone tissue is characterized by a high regenerative potential, but in the case of extensive cavities the use of implants is required, temporarily replacing its functions.

The original approach of the present work is the connection of a scaffold and a carrier of biologically active substances by placing the carrier in the form of beads or fibres in a PLA matrix to decrease the rate of protein release. The new conception of this paper is creating multifunctional composite materials able to deliver protein and also to fulfil a mechanical (constructional) function, with the proper porosity for cell migration and proliferation, and with bioactive potential. Its application to filling extensive tissue defects would give the possibility for delivery of drugs, growth factors, or other biologically active proteins (reagents). This aim was realized by creation of the novel composite materials, in which protein was incorporated in the fillers of the PLA matrix, such as PLA and alginate fibres or alginate beads. The influence of the type of polymeric carrier (fillers), their form, and the way of protein connection on albumin release were investigated. Bovine serum albumin (BSA) was applied as a model protein, a common approach in the literature [6,18,19]. Moreover, BSA gives great potential for binding reactive groups of the other compounds thanks to the free sulphydryl groups existing in the peptide chain [20]. The bioactive potential and biocompatibility of the proposed composites were also evaluated.

[Engineering of Biomaterials 169 (2023) 2-10]

doi:10.34821/eng.biomat.169.2023.2-10

Submitted: 2023-06-28, Accepted: 2023-07-19, Published: 2023-07-22

Materials and Methods

Materials

The following materials and reagents were used in the preparation of the composite samples: poly-L-lactide PLLA – Ingeo™ 3051D, NatureWorks® LLC (glass transition temperature Tg 55-65°C, molecular weight Mn 61000 g/mol, polydispersity 1.5); long poly-L-lactide fibres (fibre diameter 9.6 μm, tensile strength 1.34 GPa, Young's modulus 20.1 GPa, ε_{Fmax} 30.2%) and long calcium alginate fibres (fibre diameter 10.65 μm, tensile strength 261 MPa, Young's modulus 15.1 GPa, ε_{Fmax} 1.7%) – obtained by the wet solution method at the Department of Material and Commodity Sciences and Textile Metrology of Lodz University of Technology in Poland (the process of manufacturing fibres and their parameters are described in a previous paper [21]); bovine serum albumin (BSA) – Sigma-Aldrich; culture medium – high-glucose DMEM (4.5 g/l) with L-glutamine (Sigma-Aldrich); dichloromethane CH_2Cl_2 (Poch S.A.); TEOS (Sigma-Aldrich); 1 mol $Ca(NO_3)4H_2O$ (Sigma-Aldrich); sodium alginate (Sigma-Aldrich); $CaCl_2$ (Poch S.A.); phosphate-buffered saline – PBS (Sigma-Aldrich).

Spherical beads with BSA (1.29 mm in diameter) were formed by forcing the flow of 6% sodium alginate sol containing 1.5% BSA solution from the needle (0.5 mm) and gelling them in the 10% $CaCl_2$ solution [21].

Sample preparation

Three types of composite carriers of BSA were obtained according to the procedure described in an earlier paper [21]: (1) PPA – PLA matrix modified with PLA fibres (40 wt.%; fibres covered by protein), (2) PAA – PLA matrix modified with alginate fibres (40 wt.%; fibres covered by protein), (3) PKA – PLA matrix modified with protein-loaded alginate beads (20 wt.%).

Test methods

pH and conductivity of incubation fluids

pH and conductivity measurements were performed for 8 weeks on water extracts during incubation of the tested materials at 37°C in distilled water (DW). Before measurement, the extracts were cooled to room temperature. A CP-411M Elmetron microcomputer pH meter was used to measure pH, and a CC-315 Elmetron conductivity meter equipped with an EC-60 Elmetron electrode was used to measure conductivity.

In vitro BSA release

The samples were incubated in PBS of pH = 7.4 at 37°C for 3 weeks. A constant ratio of sample mass to PBS volume was maintained (1 g/25 ml). The *in vitro* BSA release was determined using the following steps. After a certain time, 5 ml of the supernatants were taken for testing and replaced by a fresh 5 ml of PBS. The BSA concentration of the sampled solution was determined by using a UV-vis spectrophotometer (CECIL CE2502). The absorbance was monitored at 280 nm [22,23]. The BSA concentration was calculated using a calibration curve created by known BSA concentration solutions. All samples were analysed in triplicate and expressed as the mean ± standard deviation. The value of $p < 0.05$ was regarded as statistically significant.

Microstructure and element analysis (SEM and EDS)

The samples' microstructure was determined by using a scanning electron microscope (SEM; FEI Nova NanoSEM, USA). The elements were analysed by using an X-ray energy dispersion (EDS) microanalyser coupled with a microscope. Samples were sprayed with carbon before analysis. The tests were performed for initial samples and after 4 weeks of sample incubation in PBS (pH = 7.4) and DW at 37°C.

FTIR analysis

To determine the structural changes occurring during the incubation of composites in a simulated biological environment, the initial samples and samples after 4 and 8 weeks of incubation in PBS (pH 7.4, 37°C) were examined by Fourier transform infrared spectroscopy (FTIR). The research was carried out using the transmission technique in KBr using a Bio-Rad FTS60v spectrometer. FTIR spectra were recorded in the mid-infrared in the range of 4000-400 cm^{-1}.

Cell viability assay

Determination of cell viability on the samples' surface was conducted in primary culture of human osteoblasts (NHOst; Lonza, USA). The cells were grown in plastic bottles (Nunclon, Denmark) in OGM BulletKit culture medium (Lonza, USA) with 10% calf serum FBS, in an atmosphere of 5% CO_2 and temperature of 37°C in a HeraCell incubator (Heraeus, Thermo Scientific, Germany). Cells from passage 5 were used in the culture. The cell suspension was obtained by adding 5% trypsin from EDTA (Lonza, USA). After flushing and centrifugation, the cells were brought to a concentration of 1.5×10^4 cells/ml, after which 1 ml of cell suspension was placed in wells of a 48-well culture plate (Nunclon, Denmark) containing sterile samples with a diameter of 11 mm. The positive control was the polystyrene of the bottom of the wells of the culture plate (TCPS). NHOst cell culture was carried out for 3 and 7 days. After allotted time, the cells growing on the surface of the samples were subjected to a viability test (CellTiter test), and the morphology of the cells in an optical fluorescence microscope was evaluated (Olympus, Japan). Cell tests were performed at the Faculty of Pharmacy at Jagiellonian University, Medical College in Poland.

Results and Discussion

The results of the measurements of the amount of albumin released are presented in two graphs covering the period of the first 24 hours (FIG. 1a) and the period from the first day to 3 weeks (FIG. 1b). Significant changes were observed already within the first day of incubation, especially for PPA composite, when about 29% of the concentration of the introduced protein was reached. Such a significant rate of release in the initial stage of incubation compared to other composites is because BSA was absorbed only on the surface of the fibres. In the case of alginate fibres, as a result of their swelling in the aqueous environment, protein could also be connected inside the fibres. After 2 days of PPA incubation, protein release had a linear course. These studies show that the silica–calcium sol coating does not block BSA release from PLA fibres.

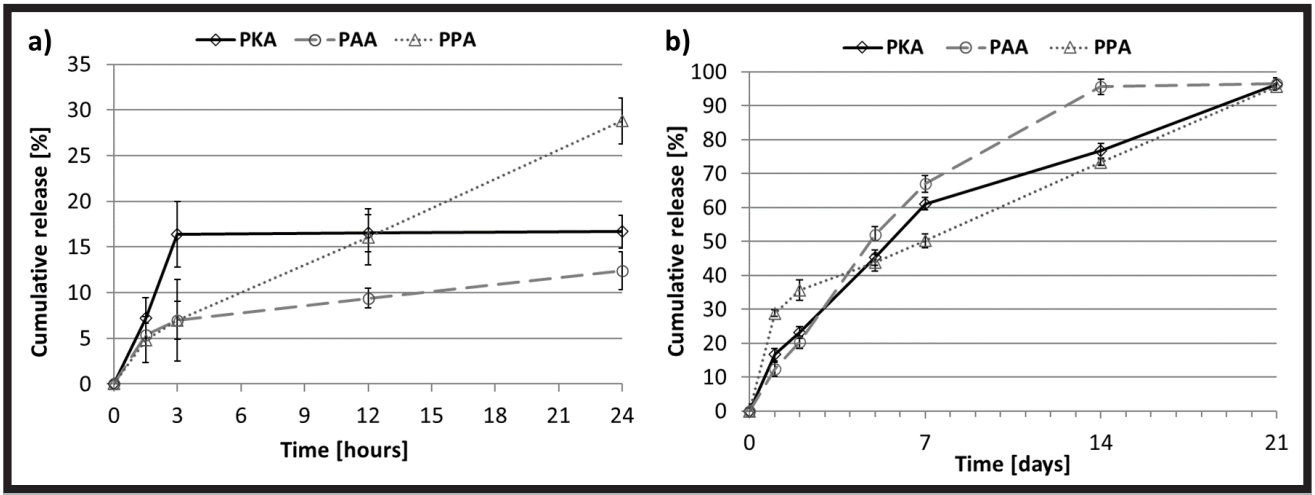

FIG. 1. Release of BSA from composites: a) during 24 h, b) during 3 weeks of incubation in PBS.

For PKA, about 17% of BSA was reached already within the first 3 hours of incubation. During the first day, the release was the slowest in the case of the PAA composite, where after 24 hours the albumin concentration was only 12%. The observed changes indicate that despite the stability of the individual phases of the composite, especially the matrix, the release of albumin begins immediately after the samples are placed in the aqueous environment. Release of albumin from the fibres' surface or alginate beads is possible thanks to the ability of the PLA matrix to absorb water and then migration of albumin in the PLA structure [24]. The rate of albumin release in the first stage of incubation can also be related to the composite's porosity and the character of PLA/modifier interfaces, which fulfil diffusion of the incubation medium and albumin (FIGs 2 and 3) [25].

The maximum protein concentration was reached after 3 weeks of incubation for all tested composites (FIG. 1b). This was confirmed by EDS analysis of the samples. In the case of the initial composites, a signal from nitrogen and sulphur from the protein was visible on the modifier's surface (FIG. 2). However, these elements were not identified after 4 weeks of incubation in PBS (FIG. 3).

Absorbance measurements showed that the rate of BSA release decreases gradually with incubation time. For alginate-carrier composites (PKA and PAA), the first stage of intensive release includes up to 1 week of incubation, during which approx. 67% of the maximum albumin content in PAA and approx. 61% of the content in PKA are released into the supernatant. For PAA, the release is the fastest, and after 2 weeks of incubation, almost the maximum concentration of the introduced protein is achieved (approx. 96%). This is due to the easier penetration of fluids through the fibre-matrix interfaces because of alginate fibres swelling and moving. The changes in alginate fibre morphology are visible in the SEM image after 4 weeks of incubation in PBS (FIG. 2b and FIG. 3b). Moreover, numerous pores can be observed. Compared to the number of pores in the initial composite, it can be seen that their number and size increased significantly after incubation. This indicates the gradual degradation of the fibres and their movement.

In the case of PKA, the protein was released gradually from hydrogel beads swelling under the influence of incubation. As shown by studies of the kinetics of BSA release from calcium alginate beads described by Nochos et al., the greater the ability to swell, the faster the BSA release process takes place [26]. This results from physical entanglements between the protein and alginate chains. At pH 7.0, alginate is in the form of a polyanion, and albumin is negatively charged; therefore, electrostatic interactions are not expected [27]. The PLA matrix hinders the swelling of alginate beads during the initial stage of incubation. On the other hand, because of drying of PKA composites, capsule shrinkage and delamination at the interface are visible in the SEM photo after 4 weeks of incubation (FIG. 3c). Unlike fibre modifications, in the case of beads, their interfaces with the matrix do not make contact with the surface of materials. Therefore, the diffusion of fluid into the interior of the composite and BSA into the incubation medium can take place mainly through the structure of the PLA matrix.

A common problem in the use of alginate carriers is too rapid release of delivered substances to the surrounding environment [7,28]. The solution proposed in this work, consisting in placing the carrier in the form of beads or fibres in the PLA matrix, effectively allows a reduction in the rate of release of the model protein. At the same time, the implant designed in this way can also perform other functions, such as a mechanical one and as a scaffold for regenerated tissue, stimulating its growth by delivering protein. As demonstrated in previous work, these composites are characterized by satisfactory mechanical properties for filling bone defects and favourable porosity due to the possibility of cell proliferation [21]. In particular, the PPA composite is characterized by a very attractive microstructure similar to that of trabecular bone (FIG. 2c). The proposed composites can be used in a situation where long-term release of the active substance is required in the treatment process.

Most apatite secretions with stoichiometry similar to that of biological apatite can be observed after 4 weeks of incubation in PBS of the PPA composite (Ca/P is 1.53) (FIG. 3a). This indicates the significant role of silica-calcium sol covering PLA fibres in the process of nucleation and growth of apatites, thus this composite has the greatest bioactive potential. EDS analysis showed the presence of silicon in the precipitates, which may suggest its incorporation into the structure and role in inducing the process of their formation. The presence of calcium phosphates was additionally confirmed by the analysis of FTIR spectra (FIG. 4), where on the PPA spectra after 4 and 8 weeks of incubation in PBS, the bands associated with vibrations of $PO4^{3-}$ groups in the range of 560-600 cm^{-1} are visible [29]. The most intense bands of phosphate groups in the range of 1020-1100 cm^{-1} overlap the C-O-C bands of PLA. However, an increase in the intensity of bands in this range after incubation compared to the spectrum of initial PPA is visible. This confirms the presence of numerous apatite secretions in the composite.

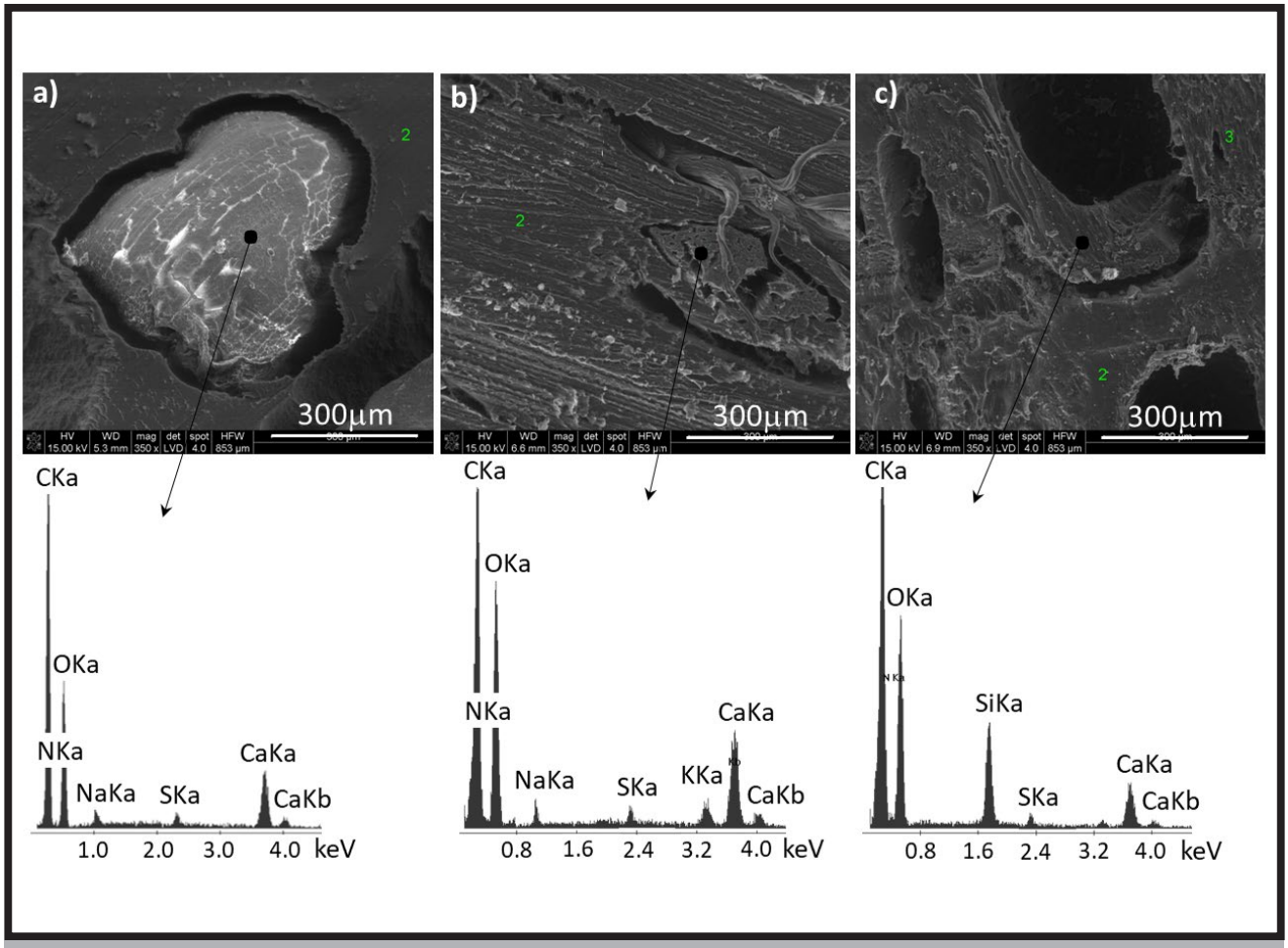

FIG. 2. SEM microstructure and EDS analysis of initial composites: a) PKA, b) PAA, c) PPA.

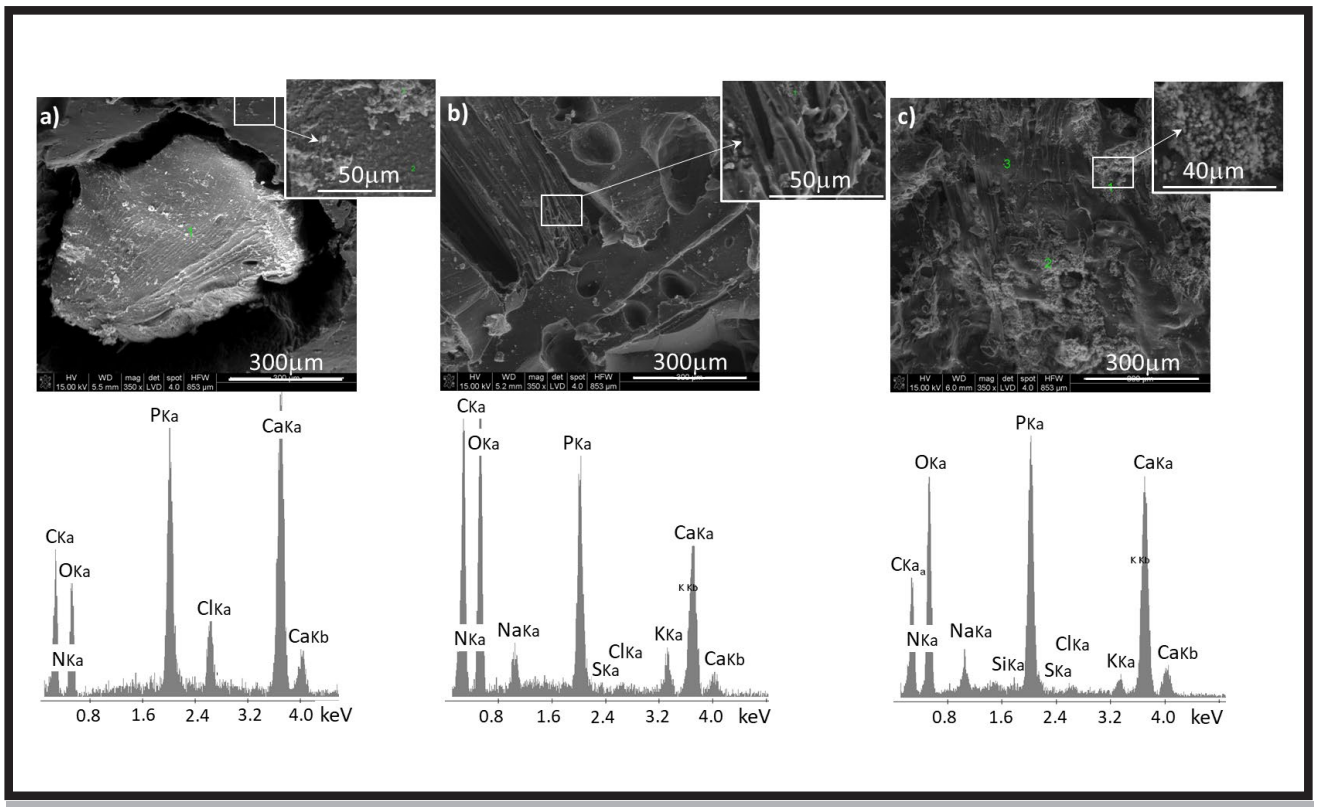

FIG. 3. SEM microstructure and EDS analysis of composites after 4 weeks of incubation in PBS: a) PKA, b) PAA, c) PPA.

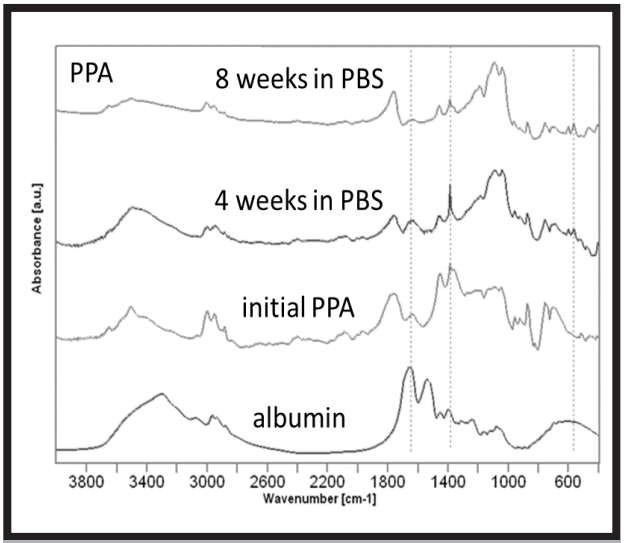

FIG. 4. FTIR spectra of albumin and PPA composite: initial and after 4 and 8 weeks of incubation in PBS.

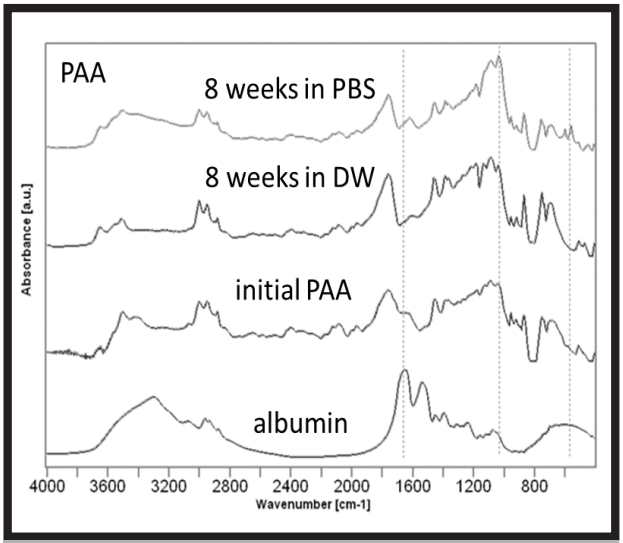

FIG. 5. FTIR spectra of albumin and PAA composite: initial and after 8 weeks of incubation in distilled water (DW) and PBS.

Importantly, calcium phosphate precipitations were present on the surface of the PAA composite after 4 weeks of incubation in PBS, although not as numerous as were visible in the case of the PPA composite (FIG. 3a). The presence of apatite was confirmed by elemental analysis. However, the molar ratio of calcium to phosphorus was 1.29 and slightly different from that typical for biological apatite (1.5-1.67). A small amount of sulphur may result from the adsorption of the released protein on the surface of the composite.

SEM images of the PKA composite after 4 weeks of incubation in PBS also allowed the observation of clearly visible calcium phosphate precipitation on the surface of the composite (FIG. 3c). Elemental analysis showed the presence of calcium to phosphorus in a ratio of 2.33, which is probably related to the increased amount of calcium derived from alginate beads.

FIGs 5 and 6 show the FTIR spectra of the PAA and PKA composites after 8 weeks of incubation in DW and PBS. No changes were observed on the spectra that could indicate degradation of PLA. However, the disappearance of the band correlated with albumin (amide I at approx. 1650 cm^{-1}), which is associated with its release (incubation in DW and PBS), can be observed. Moreover, the presence of bands connected with the $PO4^{3-}$ groups in the range of 560-600 cm^{-1} on spectra obtained for composites after incubation in PBS indicates the presence of apatite secretions. Alginate-derived bands are difficult to interpret due to the overlap of PLA and albumin bands, but after 8 weeks of incubation, the band at approx. 1620 cm^{-1} can be associated with vibrations of carboxyl groups -COOH in alginate.

The *in vitro* stability of the tested composites (especially modifiers) and the influence of modifying phases on the water environment were assessed on the basis of pH and conductivity changes of DW (FIG. 7). The measurements did not show any significant changes in pH that could indicate that the PLA degradation process had begun. This indicates that the matrix of the composites is stable in the aqueous environment during the test period (8 weeks of incubation). These results confirm previous studies on PLA degradation (PLA with the same chemical structure), which have shown that the degradation process of this polymer begins after approximately 15 weeks of incubation in DW [30].

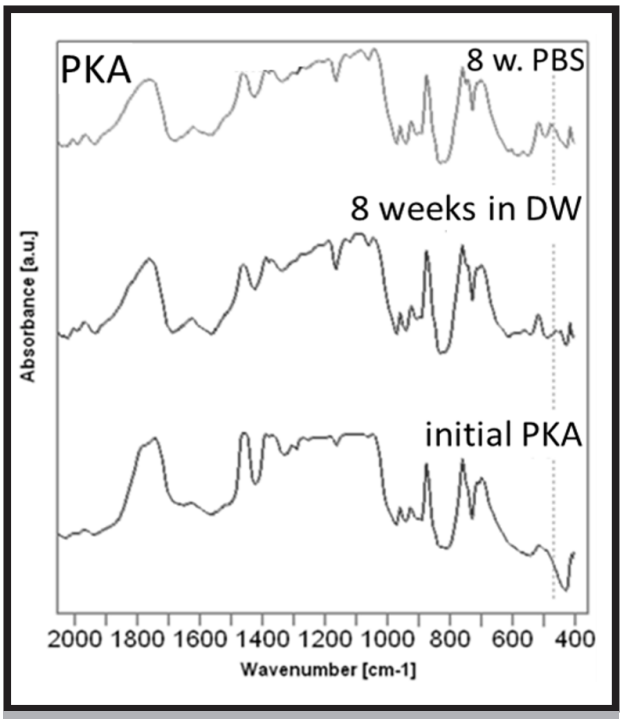

FIG. 6. FTIR spectra of PKA composite: initial and after 8 weeks of incubation in distilled water (DW) and PBS.

Despite the lack of significant changes in the pH of the supernatants, there was a visible change in their conductivity after the first day of incubation, especially in the case of the PKA and PPA composites. In the case of the PKA composite, the largest increase in conductivity occurred during the first 7 days, then the changes were gradual up to 8 weeks of incubation. As shown by the results presented above, the release of albumin occurs up to 3 weeks of incubation; therefore, an increase in conductivity after this time can be associated with partial degradation of calcium alginate. This is confirmed by the clearly smaller size of the beads visible in the SEM photo after 4 weeks of incubation in DW (FIG. 8a).

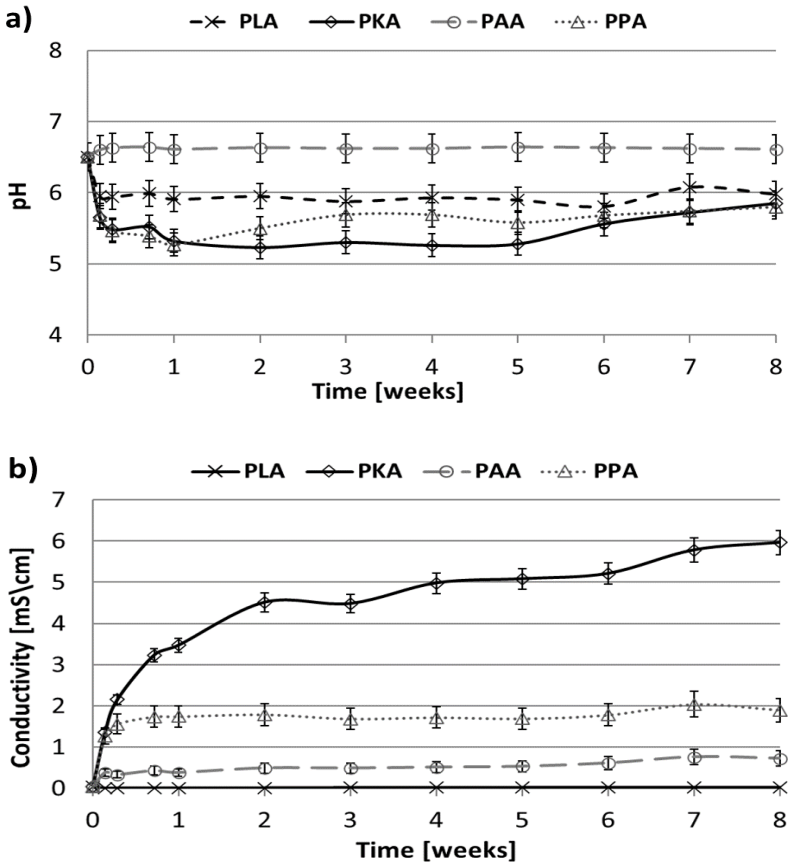

FIG. 7. Changes of pH (a) and conductivity (b) of distilled water during incubation of composites.

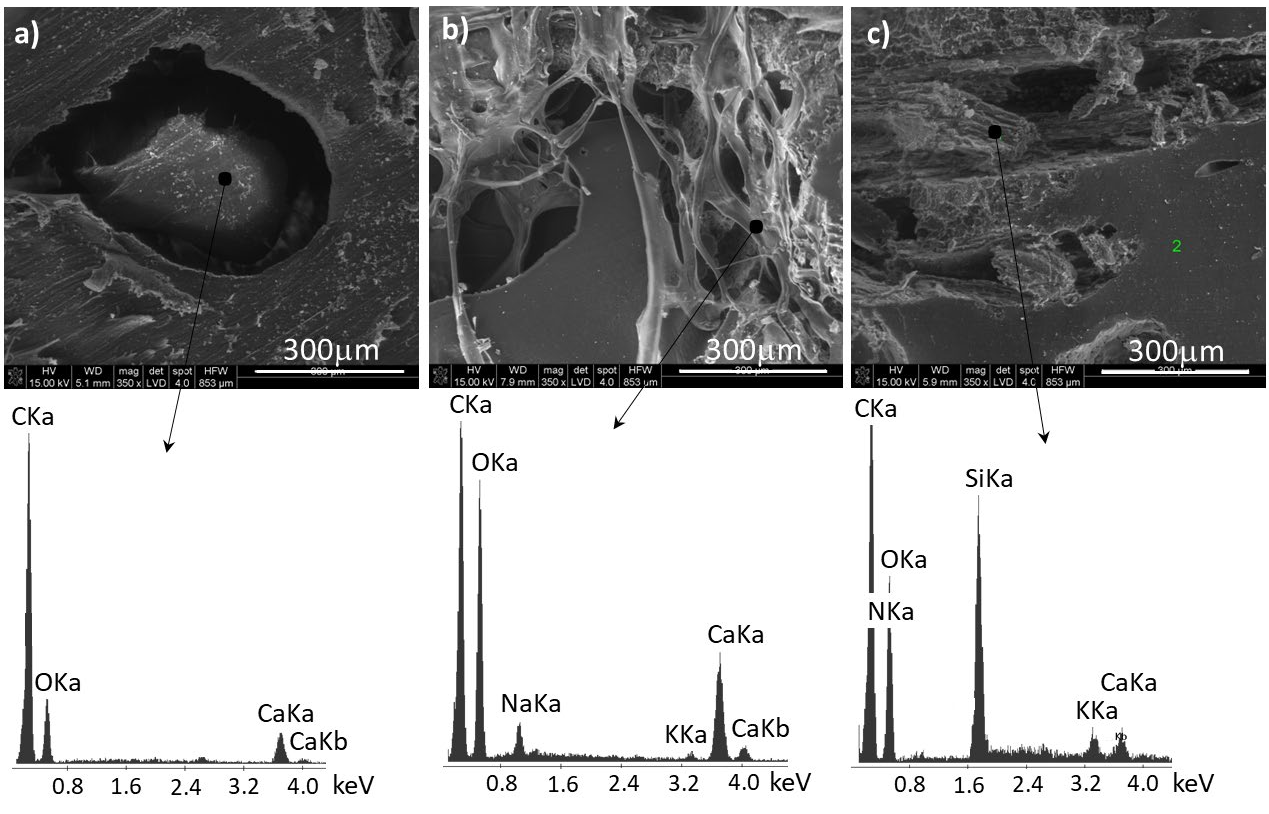

FIG. 8. SEM microstructure and EDS analysis of composites after 4 weeks of incubation in distilled water: a) PKA, b) PAA, c) PPA.

The same applies to the PPA composite. The greatest increase in conductivity occurred already on the first day of incubation, after which these changes were no longer so intense. This is largely associated with the intense release of albumin during this time: after the first day, 29% of the introduced protein was achieved (FIG. 1). In the case of the PPA composite, the increase in conductivity is associated not only with the release of albumin, but also with decomposition and release of the silica-calcium sol components. This conclusion was confirmed by the EDS analysis performed in the outer part of the fibre after 4 weeks of incubation in DW (FIG. 8c), which showed different proportions of silicon and calcium than in the sample before incubation (FIG. 2c). Importantly, the high content of silicon after 4 weeks of incubation may indicate its incorporation into the structure of the material. Moreover, the fragmentation of PLA fibres is visible in SEM images after this time. Such a rapid degradation process may be related to the influence of the solvent used during the impregnation of fibres with PLA solution on the microstructure of the fibres despite the silica-calcium sol layer used.

The weakest conductivity of incubation fluids was recorded for the PAA composite. The most significant increase in conductivity occurred after the first hour of incubation; after that, these changes were no longer so rapid and occurred gradually to the end of the measurements. The results presented by M. Boguń [31] concerning research on alginate fibres showed that the process of degradation of calcium alginate fibres in a PCL (poly-ε-caprolactone) matrix composite began after about 2 weeks of incubation, which was manifested by an increase in the conductivity of DW. These changes with 10 wt.% of fibres in the composite did not exceed 8 μS/cm. However, for the tested PAA composite, the conductivity changes were much higher. The changes in the conductivity of DW up to 3 weeks are primarily associated with the release of BSA. This was also confirmed by EDS analysis, where sulphur and nitrogen associated with the protein were present for the initial PAA composite (FIG. 2b), but after 4 weeks of incubation these elements were not detected (FIG. 8b). The slight increase in conductivity in the following weeks is probably due to the degradation of alginate fibres. Partial degradation of the fibres is confirmed by changes in the composite microstructure. A difference in the arrangement of the fibres can be observed. The fibres clearly moved and swelled during incubation and partially covered the surface of the composite. The gel form probably facilitates their migration. The influence of the environment in which the material was incubated is clearly visible. After 4 weeks of incubation in PBS, as described above, it is difficult to identify alginate fibres, but the voids left by the fibres are visible (FIG. 3b).

Cell culture showed the proper morphology of cells in contact with the surface of the composites. Cells were spread on the surface and no apoptotic cells were observed (FIG. 9). However, the most intensive cell proliferation was visible in the case of PKA composite. This was confirmed by the results of NHOst cell viability presented in FIG. 10. In the case of PAA and PKA, a significant increase in cell number between 3 and 7 days of culture is visible. The significantly lower cell viability on the composites' surface compared to the control can be associated with their porous microstructure and cell proliferation into the composite, which made it difficult to precisely analyse their quantity.

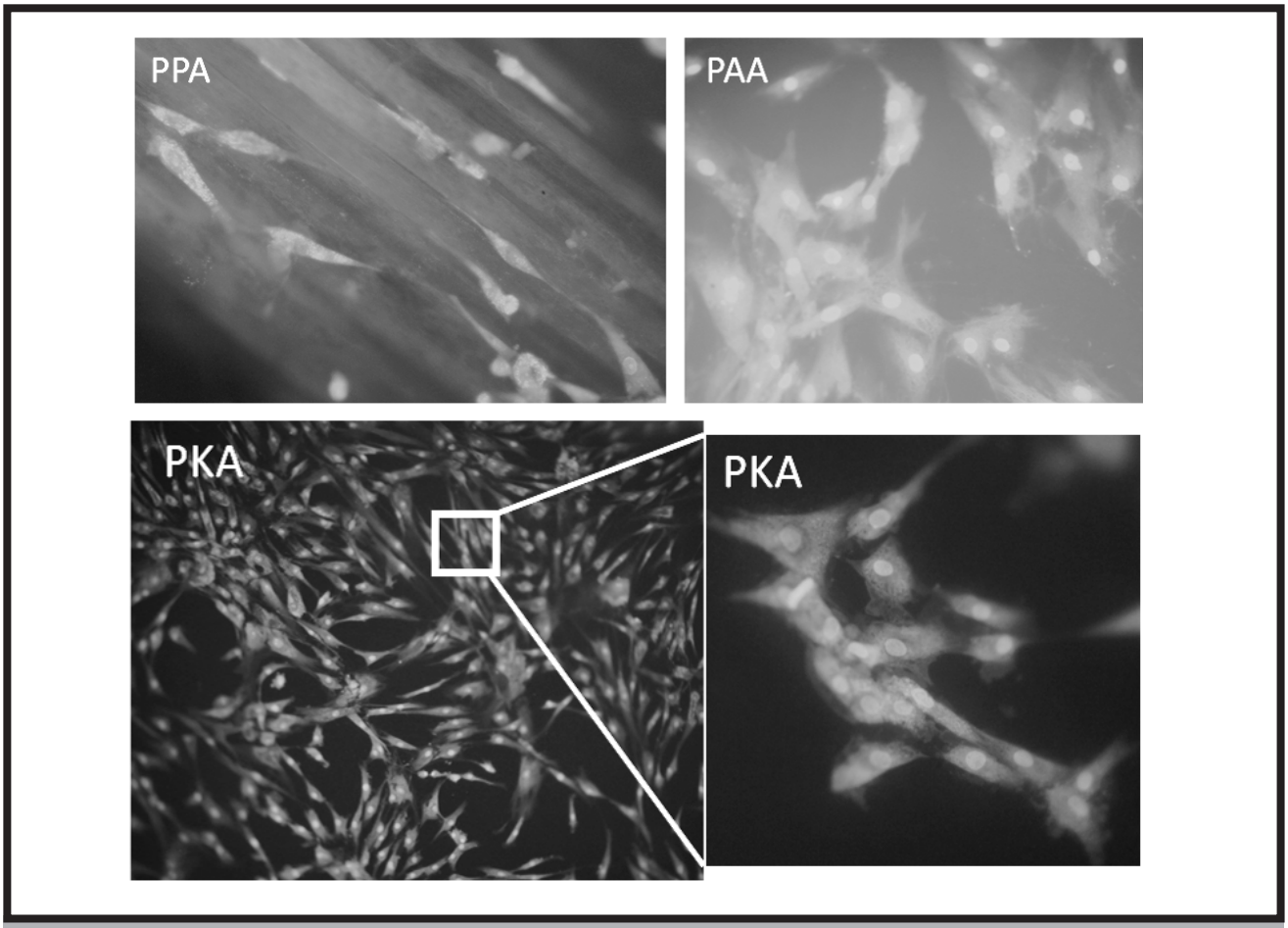

FIG. 9. Cell morphology on the composites' surface after 3 days of culture (PPA and PAA mag. 20x; PKA mag. 10x and 20x, respectively).

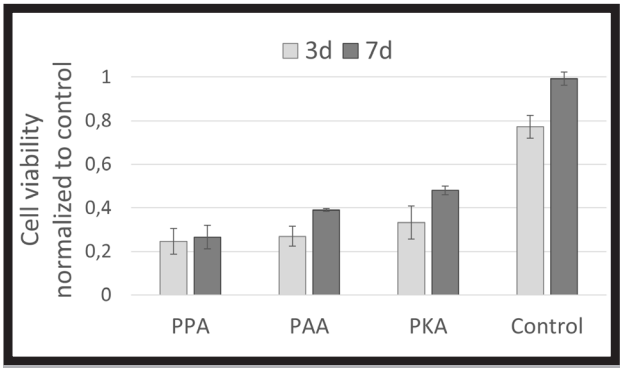

FIG. 10. NHOst cell viability determined by the CellTiter assay on days 3 and 7 of culture on the TCPS control surface and on the surfaces of the samples.

Conclusions

BSA was completely released from all tested composites during 3 weeks of incubation in PBS. The release process takes place from the first hours of incubation. Within the first day, this process is the fastest in the case of a composite with PLA fibres. This is related to only the surface adhesion of the protein on the fibres. In contrast to PLA fibres, the alginate fibres can absorb the BSA inside their volume thanks to high swelling ability in the water environment.

Studies have shown a clear difference between the forms of the alginate carrier, such as fibres or beads. The use of a fibrous form accelerates the release of protein, due to the increased number of interfaces, running along the entire length of the composite. They are fast diffusion routes allowing fluids to penetrate inside the composite and BSA to migrate outward. In the case of bead carriers, they are completely surrounded by a PLA matrix, and the interfaces do not come into contact with the environment.

In the developed composites, the degradation process begins with the carrier phases; the PLA matrix is characterized by greater stability.

All tested composites show bioactive potential connected with apatite precipitation during incubation in a simulated biological environment. The most intense growth of apatites with the optimal ratio of calcium to phosphorus can be observed for the PPA composite. This is most likely related to the presence of a silica-calcium sol stimulating the nucleation of calcium phosphates.

The cell viability test showed NHOst cell proliferation after 3 and 7 days of culture. The cells were characterized by the proper morphology. The cell viability assay indicates good biocompatibility of the tested composites.

The conception of the multifunctional role of the studied composites in potential application as bone scaffolds is summarized in FIG. 11, where the main 4 areas of their activity are presented.

Acknowledgements

This work was supported from the subsidy of the Ministry of Education and Science for the AGH University of Krakow (Project No 16.16.160.557).

Prof. Maciej Boguń (Lodz University of Technology, Department of Material and Commodity Sciences and Textile Metrology, Poland) for polylactide and alginate fibres manufacturing, Elżbieta Menaszek Ph.D. (Jagiellonian University, Medical College, Faculty of Pharmacy, Poland) for performing cell tests (including photos of cells) with a description of the research method and Agnieszka Daszyńska (AGH University of Krakow, Faculty of Materials Science and Ceramics, Department of Biomaterials and Composites, Poland) for help in data acquisition are gratefully acknowledged.

ORCID iD

A. Morawska-Chochół: https://orcid.org/0000-0003-0209-4402

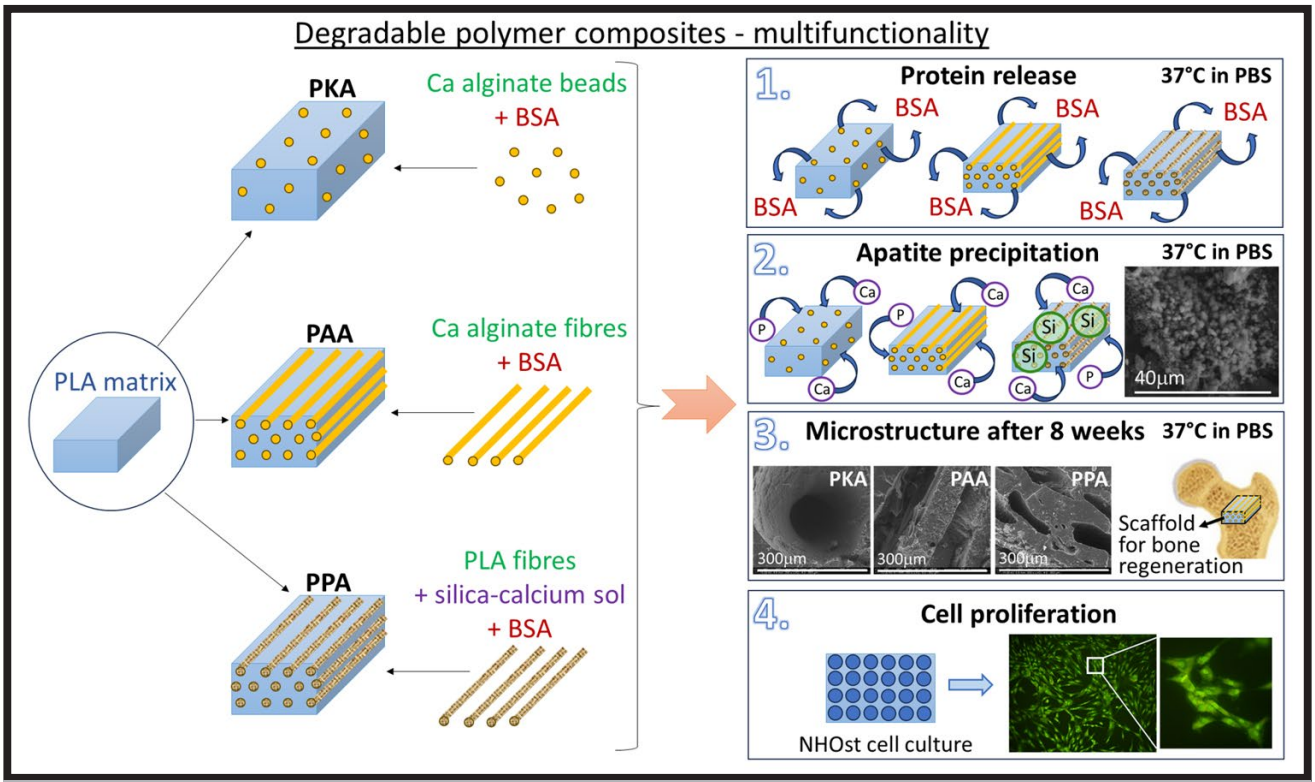

FIG. 11. Graphical summary of the results: scaffolds composition and the main areas of their activity.

References

[1] Dorogin J., Townsend J.M., Hettiaratchi M.H.: Biomaterials for protein delivery for complex tissue healing responses. Biomaterials Science 9 (2021) 2339-2361. http://doi.org/10.1039/d0bm01804j

[2] Echeverria Molina M.I., Malollari K.G., Komvopoulos K.: Design challenges in polymeric scaffolds for tissue engineering. Frontiers in Bioengineering and Biotechnology 9 (2021) 617141. http://doi.org/10.3389/fbioe.2021.617141

[3] Zhao D., Zhu T., Li J., Cui L., Zhang Z., Zhuang, X., Ding J.: Poly(lactic-co-glycolic acid)-based composite bone-substitute materials. Bioactive Materials 6 (2021) 346-360. http://doi.org/10.1016/j.bioactmat.2020.08.016

[4] Sheng Y., Gao J., Yin Z.Z., Kang J., Kong Y.: Dual-drug delivery system based on the hydrogels of alginate and sodium carboxymethyl cellulose for colorectal cancer treatment. Carbohydrate Polymers 269 (2021) 118325. http://doi.org/10.1016/j.carbpol.2021.118325

[5] Li H., Li P., Yang Z., Gao C., Fu L., Liao Z., Zhao T., et al.: Meniscal regenerative scaffolds based on biopolymers and polymers: Recent Status and Applications. Frontiers in Cell and Developmental Biology 9 (2021) 661802. http://doi.org/10.3389/fcell.2021.661802

[6] Pakulska M.M., Donaghue I.E., Obermeyer J.M., Tuladhar A., McLaughlin C.K., Shendruk T.N., Shoichet M.S.: Encapsulation-free controlled release: Electrostatic adsorption eliminates the need for protein encapsulation in PLGA nanoparticles. Science Advances 2 (2016) e1600519. http://doi.org/10.1126/sciadv.1600519

[7] Yao B., Ni C., Xiong C., Zhu C., Huang B.: Hydrophobic modification of sodium alginate and its application in drug controlled release. Bioprocess and Biosystems Engineering 33:4 33 (2009) 457-463. http://doi.org/10.1007/S00449-009-0349-2

[8] Lee B.K., Yun Y., Park K.: PLA micro- and nano-particles. Advanced Drug Delivery Reviews 107 (2016) 176. http://doi.org/10.1016/j.addr.2016.05.020

[9] Brzeziński M., Wedepohl S., Kost B., Calderón M.: Nanoparticles from supramolecular polylactides overcome drug resistance of cancer cells. European Polymer Journal 109 (2018) 117-123. http://doi.org/10.1016/J.EURPOLYMJ.2018.08.060

[10] Marincaș L., Farkas N.I., Barbu-Tudoran L., Barabás R., Toşa M.I.: Deep eutectic solvent PCL-based nanofibers as drug delivery system. Materials Chemistry and Physics 304 (2023) 127862. http://doi.org/10.1016/J.MATCHEMPHYS.2023.127862

[11] Li J., Ding J., Liu T., Liu J.F., Yan L., Chen X.: Poly(lactic acid) controlled drug delivery. In Industrial Applications of Poly(lactic acid). Advances in Polymer Science; Di Lorenzo, M., Androsch, R., Eds.; Springer: New York (2017); Vol. 282, pp. 109-138.

[12] Liu S., Qin S., He M., Zhou D., Qin Q., Wang H.: Current applications of poly(lactic acid) composites in tissue engineering and drug delivery. Composites Part B: Engineering 199 (2020) 108238. http://doi.org/10.1016/j.compositesb.2020.108238

[13] Sharma S., Gupta V., Mudgal D.: Experimental investigations on polydopamine coated poly lactic acid based biomaterial fabricated using 3D printing for orthopedic applications. Materials Chemistry and Physics 310 (2023) 128473. http://doi.org/10.1016/J.MATCHEMPHYS.2023.128473

[14] Pyza M., Brzezińska N., Kulińska K., Gabor J., Barylski A., Aniołek K., et al.: Polylactide-based composite materials for 3D printing and medical applications - the effect of basalt and silicon dioxide addition. Engineering of Biomaterials 166 (2022) 29-39. http://doi.org/10.34821/eng.biomat.166.2022.29-39

[15] Senatov F.S., Zadorozhnyy M.Y., Niaza K.V., Medvedev V.V., Kaloshkin S.D., Anisimova N.Y., Kiselevskiy M.V., Yang K.C.: Shape memory effect in 3D-printed scaffolds for self-fitting implants. European Polymer Journal 93 (2017) 222-231. http://doi.org/10.1016/J.EURPOLYMJ.2017.06.011

[16] Kumawat V.S., Bandyopadhyay-Ghosh S., Ghosh S.B.: Rationally designed biomimetic bone scaffolds with hierarchical porous-architecture: Microstructure and mechanical performance. Express Polymer Letters 17 (2023) 610-624. http://doi.org/10.3144/expresspolymlett.2023.45

[17] Gryń K.: Long-term mechanical testing of multifunctional composite fixation miniplates. Engineering of Biomaterials 157 (2020) 20-25. http://doi.org/10.34821/eng.biomat.157.2020.20-25

[18] Yadav P., Yadav B.: Preparation and characterization of BSA as a model protein loaded chitosan nanoparticles for the development of protein-/ peptide-based drug delivery system. Future Journal of Pharmaceutical Sciences 7 (2021) 200. http://doi.org/10.1186/s43094-021-00345-w

[19] Norudin N.S., Mohamed H.N., Yahya N.A.M.: Controlled released alginate-inulin hydrogel: Development and in-vitro characterization. AIP Conference Proceedings 2016 (2018) 20113. http://doi.org/10.1063/1.5055515

[20] Yang Z., Cui Y., Zhang Y., Liu P., Zhang Q., Zhang B.: Identification of imprinted sites by fluorescence detection method based on reversible dynamic bond modified template protein. Composites Part B: Engineering 223 (2021) 109154. http://doi.org/10.1016/j.compositesb.2021.109154

[21] Morawska-Chochół A.: Manufacturing of resorbable composite biomaterials containing protein. Materials and Manufacturing Processes 37 (2022) 782-791. http://doi.org/10.1080/10426914.2021.2001508

[22] Tang L., Chen Y.H., Wang Q., Wang X.H., Wu Q.X., Ding Z.F.: Microencapsulation of functional ovalbumin and bovine serum albumin with polylysine-alginate complex for sustained protein vehicle's development. Food Chemistry 368 (2022) 130902. http://doi.org/10.1016/j.foodchem.2021.130902

[23] Noble J.E.: Quantification of protein concentration using UV absorbance and Coomassie dyes. Methods in Enzymology 536 (2014) 17-26. http://doi.org/10.1016/B978-0-12-420070-8.00002-7

[24] Ilyas R.A., Sapuan S.M., Harussani M.M., Hakimi M.Y.A.Y., Haziq M.Z.M., Atikah M.S.N., Asyraf M.R.M., Ishak M.R., Razman M.R., Nurazzi N.M., Norrrahim M.N.F., Abral H., Asrofi M.: Polylactic acid (PLA) biocomposite: Processing, additive manufacturing and advanced applications. Polymers 13 (2021) 1326. http://doi.org/10.3390/polym13081326

[25] Amini M., Khavandi A.: Degradation of polymer-based composites in corrosive media: experimental attempts towards underlying mechanisms. Mechanics of Time-Dependent Materials 23 (2019) 153-172. http://doi.org/10.1007/S11043-018-09408-7

[26] Nochos A., Douroumis D., Bouropoulos N.: In vitro release of bovine serum albumin from alginate/HPMC hydrogel beads. Carbohydrate Polymers 74 (2008) 451-457. http://doi.org/10.1016/j.carbpol.2008.03.020

[27] Wells L.A., Sheardown H.: Extended release of high p*I* proteins from alginate microspheres via a novel encapsulation technique. European Journal of Pharmaceutics and Biopharmaceutics 65 (2007) 329-335. http://doi.org/10.1016/j.ejpb.2006.10.018

[28] Ko C.L., Wu H.Y., Lin Y.S., Yang C.H., Chen J.C., Chen W.C.: Modulating the release of proteins from aloaded carrier of alginate/gelatin porous spheres immersed in different solutions. Bio-Medical Materials and Engineering 28 (2017) 515-529. http://doi.org/10.3233/BME-171690

[29] Abifarin J.K., Obada D.O., Dauda E.T., Dodoo-Arhin D.: Experimental data on the characterization of hydroxyapatite synthesized from biowastes. Data in Brief 26 (2019) 104485. http://doi.org/10.1016/j.dib.2019.104485

[30] Chłopek J., Morawska-Chochół A., Szaraniec B.: The influence of the environment on the degradation of polylactides and their composites. Journal of Achievements in Materials and Manufacturing Engineering 43 (2010) 72-79. https://api.semanticscholar.org/CorpusID:137640086

[31] Boguń M., Krucińska I., Kommisarczyk A., Mikołajczyk T., Błażewicz M., Stodolak-Zych E., Menaszek E., Ścisłowska-Czarnecka A.: Fibrous polymeric composites based on alginate fibres and fibres made of poly-ε-caprolactone and dibutyryl chitin for use in regenerative medicine. Molecules 18 (2013) 3118-3136. http://doi.org/10.3390/molecules18033118